Interactions of organosulfates with water vapor under sub- and supersaturated conditions

Chao Peng,[1,2] Patricia N. Razafindrambinina,[3] Kotiba A. Malek,[4] Lanxiadi Chen,[1,2,7] Weigang Wang,[5] Ru-Jin Huang,[6] Yuqing Zhang,[1,2] Xiang Ding,[1,2] Maofa Ge,[5] Xinming Wang,[1,2] Akua A. Asa-Awuku,[3,4] and Mingjin Tang[1,2,7,*]

[1] State Key Laboratory of Organic Geochemistry, Guangdong Key Laboratory of Environmental Protection and Resources Utilization, and Guangdong-Hong Kong-Macao Joint Laboratory for Environmental Pollution and Control, Guangzhou Institute of Geochemistry, Chinese Academy of Sciences, Guangzhou 510640, China

[2] CAS Center for Excellence in Deep Earth Science, Guangzhou 510640, China

[3] Department of Chemistry and Biochemistry, College of Computer, Mathematical and Natural Sciences, University of Maryland, College Park, MD 20742, USA

[4] Department of Chemical and Biomolecular Engineering, A. James Clark School of Engineering, University of Maryland, College Park, MD 20742, USA

[5] State Key Laboratory for Structural Chemistry of Unstable and Stable Species, Beijing National Laboratory for Molecular Sciences, CAS Research/Education Center for Excellence in Molecular Sciences, Institute of Chemistry, Chinese Academy of Sciences, Beijing 100190, China

[6] Key Laboratory of Aerosol Chemistry and Physics, State Key Laboratory of Loess and Quaternary Geology, Institute of Earth and Environment, Chinese Academy of Sciences, Xi'an 710061, China

[7] University of Chinese Academy of Sciences, Beijing 100049, China

*Correspondence: Mingjin Tang (mingjintang@gig.ac.cn)

Abstract

Organosulfates (OS) are important constituents of secondary organic aerosols, but their hygroscopic properties and cloud condensation nucleation (CCN) activities have not been well understood. In this work we employed three complementary techniques to characterize interactions of several OS with water vapor under sub- and supersaturated conditions. A vapor sorption analyzer was used to measure mass changes of OS samples with RH (0-90%); among the 11 organosulfates examined, only sodium methyl sulfate (methyl-OS), sodium ethyl sulfate (ethyl-OS), sodium octyl sulfate (octyl-OS) and potassium hydroxyacetone sulfate were found to deliquesce as RH increased, and their mass growth factors at 90% RH were determined to be 3.65 ±0.06, 3.58 ±0.02, 1.59 ±0.01 and 2.20 ±0.03. Hygroscopic growth of methyl-, ethyl- and octyl-OS aerosols was also studied using a humidity tandem differential mobility analyzer (H-TDMA); continuous hygroscopic growth was observed, and their growth factors at 90% RH were determined to be 1.83 ±0.03, 1.79 ±0.02 and 1.21 ±0.02. We further investigated CCN activities of methyl-, ethyl- and octyl-OS aerosols, and their single hygroscopicity parameters (κ_{ccn}) were determined to be 0.459 ±0.021, 0.397 ±0.010 and 0.206 ±0.008. For methyl- and ethyl-OS aerosols, κ_{ccn} values agree reasonably well with those derived from H-TDMA measurements (κ_{gf}) with relative differences being <25%, whereas κ_{ccn} was found to be ~2.4 times larger than κ_{gf} for octyl-OS, likely due to both solubility limit and surface tension reduction.

1 Introduction

Secondary organic aerosol (SOA) contributes approximately 70% to the global atmospheric organic aerosols (Hallquist et al., 2009; Jimenez et al., 2009). SOA can affect the Earth's radiative forcing and climate directly by scattering and absorbing solar and terrestrial radiation, and also indirectly by acting as cloud condensation nuclei (CCN) or ice nucleating particles (Moise et al., 2015; Shrivastava et al., 2017). Consequently, it is important to understand the source, formation, and physicochemical properties of SOA (Pöschl, 2005; Jimenez et al., 2009; Noziere et al., 2015; Peng et al., 2020). However, SOA concentrations on the global scale are significantly underestimated by many modeling studies (Heald et al., 2005; Kanakidou et al., 2005; Ervens et al., 2011; McNeill et al., 2012; Shrivastava et al., 2017), indicating that there might exist unknown while important precursors and/or formation mechanisms of SOA.

Organosulfates (OS), which could contribute to the total mass of ambient organic aerosols by as much as 30%, may largely explain the discrepancy between observed and modeled global SOA budgets (Surratt et al., 2008; Tolocka and Turpin, 2012; Liao et al., 2015). A number of field measurements have observed significant amounts of OS in ambient aerosols in different regions over the globe (Froyd et al., 2010; Kristensen and Glasius, 2011; He et al., 2014; Hettiyadura et al., 2015; Riva et al., 2019; Wang et al., 2019a; Wang et al., 2019b; Zhang et al., 2019; Bruggemann et al., 2020; Wang et al., 2020). For example, the mass concentration of sodium methyl sulfate, the smallest organosulfate, was found to be 0.2-9.3 ng m^{-3} in Centreville, Alabama (Hettiyadura et al., 2017). Hydroxyacetone sulfate, which may originate from both biogenic (Surratt et al., 2008) and anthropogenic emissions (Hansen et al., 2014), has been detected at various locations, such as the Arctic (1.27-9.56 ng m^{-3}) (Hansen et al., 2014), Beijing (0.5-7.5 ng m^{-3}) (Wang et al., 2018), Shanghai (1.8-2.3 ng m^{-3}) (Wang et al., 2021), Xi'an (0.9-2.6 ng m^{-3})

(Huang et al., 2018), Centreville (1.5-14.3 ng m^{-3}) (Hettiyadura et al., 2017) and Iowa City (4.8 ±1.1 ng m^{-3}) (Hughes and Stone, 2019). In addition, benzyl and phenyl sulfates were also ubiquitous in the troposphere, with reported concentrations up to almost 1 μg m^{-3} (Kundu et al., 2013; Ma et al., 2014; Staudt et al., 2014; Huang et al., 2018).

As OS are ubiquitous in the troposphere, it is important to understand their hygroscopic properties and CCN activities in order to assess their environmental and climatic effects (Kanakidou et al., 2005; Moise et al., 2015; Tang et al., 2016; Tang et al., 2019a), especially considering that OS could contribute up to 30% of total mass of organic aerosols in the troposphere (Surratt et al., 2008; Tolocka and Turpin, 2012; Liao et al., 2015). However, to our knowledge, only two previous studies have explored their hygroscopic properties and CCN activities (Hansen et al., 2015; Estillore et al., 2016). Hansen et al. (2015) investigated hygroscopic growth and CCN activation of limonene-derived OS (with molecular weight of 250 Da) and their mixtures with ammonium sulfate. Hygroscopicity of pure limonene-derived OS was weak, and its hygroscopic growth factors were determined to be 1.0 at 80% RH and 1.2 at 93% RH (Hansen et al., 2015). Estillore et al. (2016) investigated hygroscopic growth of a series of OS, including potassium salts of glycolic acid sulfate, hydroxyacetone sulfate, 4-hydroxy-2,3-epoxybutane sulfate, and 2-butenediol sulfate, as well as sodium salts of benzyl sulfate, methyl sulfate, ethyl sulfate, and propyl sulfate. Continuous hygroscopic growth (i.e. without obvious deliquescence) was observed for these OS aerosols (Estillore et al., 2016); in addition, their hygroscopic growth factors at 85% RH were determined to vary between 1.29 and 1.50, suggesting that their hygroscopicity showed substantial variation. In summary, it is fair to state that hygroscopic properties and CCN activities of OS have not been well understood.

In this work, three complementary techniques were used to investigate hygroscopic properties and CCN activities of a series of OS, including sodium methyl sulfate, sodium ethyl sulfate, sodium octyl sulfate, sodium dodecyl sulfate, potassium hydroxyacetone sulfate, potassium 3-hydroxy phenyl sulfate, potassium benzyl sulfate, potassium 2-methyl benzyl sulfate, potassium 3-methyl benzyl sulfate, potassium 2,4-dimethyl benzyl sulfate and potassium 3,5-dimethyl benzyl sulfate. A vapor sorption analyzer was employed to measure mass change of these OS samples as a function of RH. In addition, hygroscopic growth (change in mobility diameters) and CCN activation of submicron aerosol particles were studied for sodium methyl sulfate, sodium ethyl sulfate and sodium octyl sulfate, using a humidity tandem differential mobility analyzer (H-TDMA) and a cloud condensation nuclei counter (CCNc). Due to their very limited quantities, we could not carry out H-TDMA and CCNc measurements for other OS samples which were synthesized by us. In addition, we also investigated the impacts of sodium methyl sulfate, sodium ethyl sulfate and sodium octyl sulfate on hygroscopic properties and CCN activities of ammonium sulfate.

2 Experimental section

2.1 Chemicals and reagents

Sodium methyl sulfate (CH_3SO_4Na, >98%) and sodium ethyl sulfate ($C_2H_5SO_4Na$, >98%) were purchased from Tokyo Chemical Industry (TCI); sodium octyl sulfate ($C_8H_{17}SO_4Na$, >99%), sodium dodecyl sulfate ($C_{12}H_{25}SO_4Na$, >99%) and ammonium sulfate (>99.5%) were supplied by Aldrich. The other seven OS, including potassium hydroxyacetone sulfate, potassium 3-hydroxy phenyl sulfate, potassium benzyl sulfate, potassium 2-methyl benzyl sulfate, potassium 3-methyl benzyl sulfate, potassium 2,4-dimethyl benzyl sulfate and potassium 3,5-dimethyl benzyl sulfate, were synthesized using the method described by Huang et al. (2018), and their purities were found

to be >95% using nuclear magnetic resonance analysis. Chemical formulas and molecular structures of OS investigated in this study can be found in Figure 1.

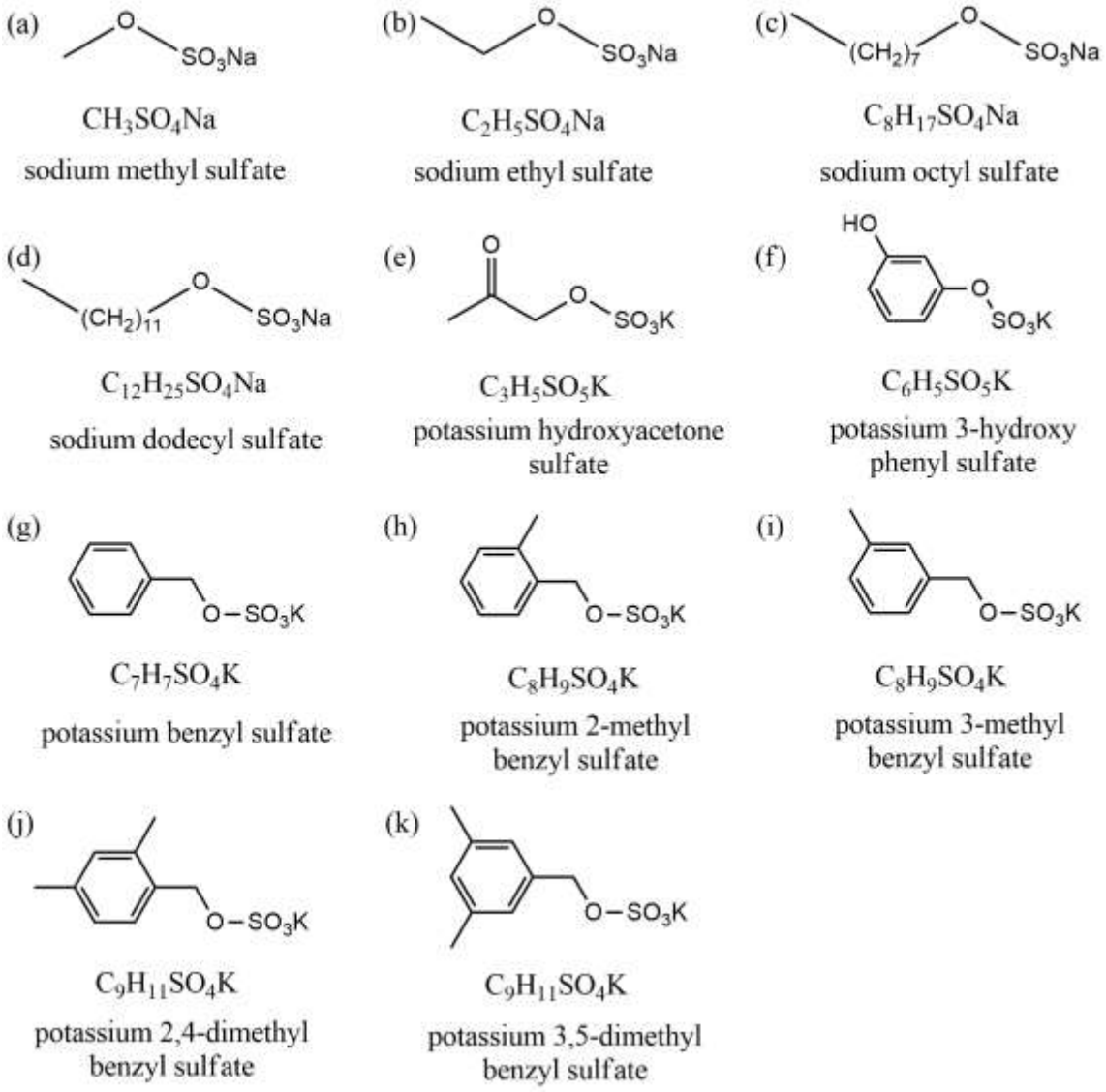

Figure 1. Chemical formulas and molecular structures of organosulfates investigated in this study.

2.2 VSA experiments

A vapor sorption analyzer (VSA), commercialized by TA Instruments (New Castle, DE, USA), was used to measure mass change of organosulfates as a function of RH. Experimental

details can be found in our previous studies (Chen et al., 2019; Gu et al., 2017; Guo et al., 2019; Tang et al., 2019b), and are thus described here briefly. Experiments were conducted at 25±0.1 °C and in the RH range of 0-90%. A high precision balance was used to measure the sample mass at different RH with a stated sensitivity of <0.1 μg, and the dry mass of samples used in this work was typically around 1.0 mg.

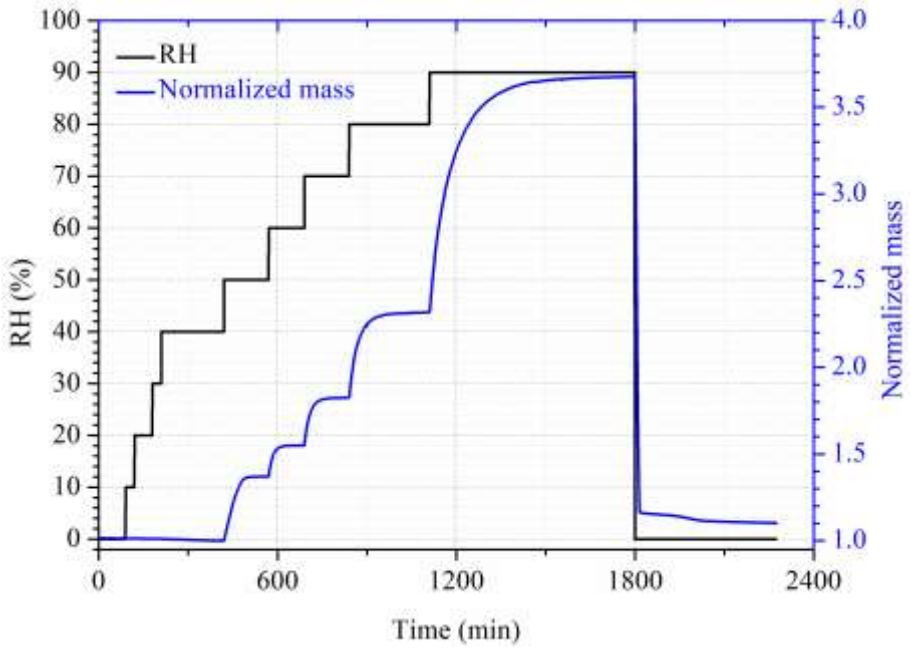

Figure 2. Change in RH (black curve, left *y* axis) and normalized sample mass (blue curve, right *y* axis) of CH_3SO_4Na with of time in a typical vapor sorption analyzer experiment at 25 °C.

As shown in Figure 2, the mass of OS samples at different RH was determined by the VSA using the following method. RH was set to <1% to dry the sample; after the sample mass was stabilized, RH was increased to 90% stepwise with an interval of 10% per step; at the end, RH was changed back to <1% to dry the sample again. The sample was considered to reach the equilibrium at a given RH when the mass change was measured to be <0.1% within 30 min. All the experiments

were conducted at least three times in our work. The sample mass at a given RH (m) was normalized to that at <1% RH (m_0) to determine the mass growth factor, defined as m/m_0.

2.3 H-TDMA experiments

A custom-built hygroscopicity tandem differential mobility analyzer (H-TDMA) was used to measure the mobility diameters of OS aerosol particles at different RH (5-90%) at 24 ±1 °C. The instrument was detailed elsewhere (Jing et al., 2016; Peng et al., 2016), and therefore only a brief introduction is given here. A commercial atomizer (MSP 1500) was used to produced polydisperse aerosol particles from dilute OS solutions in water (around 0.1 wt %), and the generated aerosol was dried to <5% RH by passing the aerosol flow through a Nafion dryer (MD-110-12S) and then a silica gel diffusion dryer. The dry aerosol flow was subsequently split to two flows. One aerosol flow was sent to the vent, and the other aerosol flow (0.3 L min^{-1}) was passed through the first differential mobility analyzer (DMA) to produce quasi-monodisperse aerosol particles with a mobility diameter of 100 nm. After that, the aerosol flow was humidified to a desired RH by flowing through a humidification section, which was made of two Nafion tubes (MD-700-12F-1) connected in series, and the residence time in the humidification section was ~27 s. Finally, the size distribution of humidified aerosol was measured by a scanning mobility particle sizer (SMPS), which consisted of the second DMA coupled to a condensation particle counter (CPC 3776, TSI). RH of the aerosol flow and the sheath flow in the second DMA were maintained to be equal and monitored using a commercial dew-point hygrometer (Michell, UK) with a stated uncertainty of ±0.08% RH. In addition, the flow rate ratio of the sheath flow to the aerosol flow was set to 10:1 for both DMAs.

Hygroscopic growth factors (GF), defined as d/d_0 (d is the mobility diameter at a given RH and d_0 is the mobility diameter at RH <5%) were reported. All the experiments were conducted in

triplicate. During our experiments, ammonium sulfate was used to calibrate the H-TDMA system routinely, and the absolute differences between the measured and theoretical GF at 90% RH were found to be within 0.04, confirming the robustness of our measurements.

2.4 CCN experiments

The CCN activity of aerosol particles was determined using a commercial cloud condensation nuclei counter (CCNc, CCN-100, Droplet Measurement Technologies, Longmont, CO, USA) described in previous studies (Roberts and Nenes, 2005; Lance et al., 2006; Moore et al., 2010). Polydisperse aerosol particles were generated using a commercial atomizer (TSI 3076), in which concentrations of solutions used were around 0.1 g/L. The wet aerosol flow generated was passed through two silica gel diffusion dryers to reduce its RH to <5% RH. After that, a dry aerosol flow (~800 mL min^{-1}) was passed through a DMA (TSI 3081) in size scanning mode to produce quasi-monodisperse aerosols, and subsequently the aerosol flow was split to two streams: one stream (~300 mL/min) was sampled into a commercial CPC (TSI 3775) to measure total number concentrations of aerosol particles ([CN]), and the second flow (~500 mL/min) was sampled into the cloud condensation nuclei counter (CCNc, CCN-100) to measure number concentrations of CCN ([CCN]).

Activation fractions ([CCN]/[CN]) of size-resolved dry particles were determined using the Scanning Mobility CCN Analysis (SMCA) method described elsewhere (Moore et al., 2010). In brief, the DMA was operated in the scanning voltage mode, and thus one activation curve (activation fractions as a function of dry diameter) could be obtained in 60-120s. The multiple charge effect was also corrected in this method, and in our work the supersaturation (*SS*) was set in the range of 0.45-1.13% with the stated uncertainty to be ±0.01%. As shown in Figure 3, activation fractions of sodium methyl sulfate (methyl-OS) and its internally mixed aerosol with

ammonium sulfate were measured at four different SS with dry mobility diameters between 20 and 100 nm. Activation fractions were fitted versus dry diameters, and the critical particle diameter (d_{50}) was determined as the dry diameter at which the activation fraction is equal to 0.5. During our measurements, ammonium sulfate was used to calibrate supersaturations, and the Pitzer-ion interaction model was applied in the calibration procedure to account for incomplete dissociation of ammonium sulfate at droplet activation (Pitzer and Mayorga, 1973; Clegg and Brimblecombe, 1988). The corrected supersaturations were reported in our work.

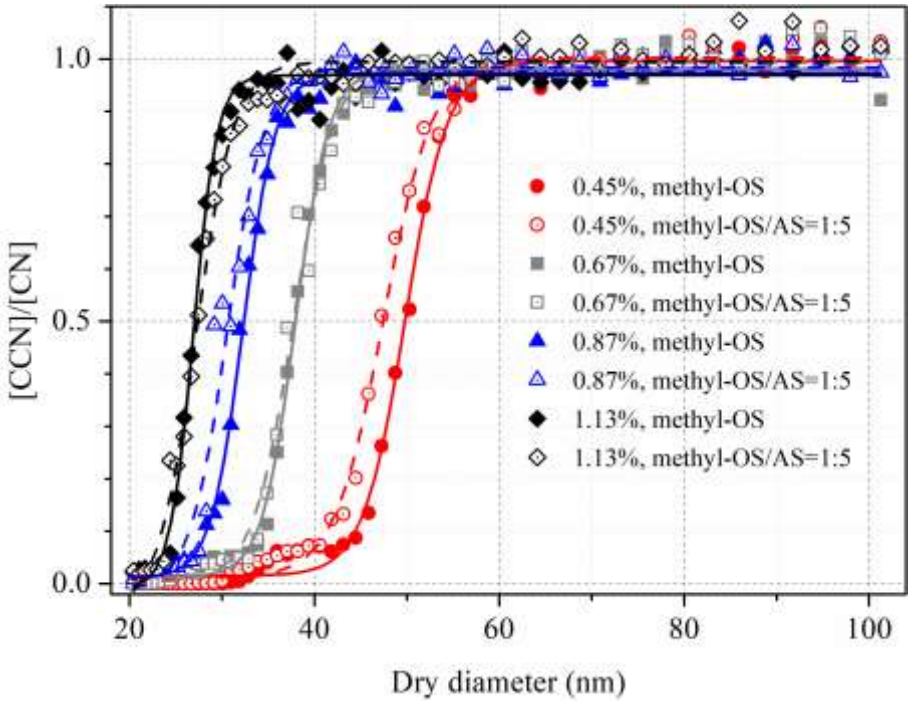

Figure 3. Activation fractions of methyl-OS and its internally mixed aerosol particles with ammonium sulfate (AS) as a function of dry particle diameter at four supersaturations.

3 Results and discussion

3.1 Mass growth of organosulfates

Figure 4 displays mass growth factors of sodium methyl sulfate (methyl-OS), sodium ethyl sulfate (ethyl-OS), sodium octyl sulfate (octyl-OS), sodium dodecyl sulfate (dodecyl-OS) and potassium hydroxyacetone sulfate, and the data are also listed in Table 1. Figure 4a suggests that methyl-OS was deliquesced when RH was increased from 40% to 50%, and after that mass growth factors increased further with RH. The mass of ethyl-OS was moderately increased (by ~11%) when RH was increased from 40% to 50%, and further increase in RH to 60% led to additional while small increase in sample mass (by ~2%); the increase in sample mass at 50% and 60% RH may be because ethyl-OS were partially deliquesced at this stage. When RH was increased to 70%, ethyl-OS was completely deliquesced, and further increase in RH (to 80% and 90%) resulted in further increase in sample mass. Octyl-OS was only deliquesced when RH was increased from 80% to 90%, whereas no significant water uptake was observed for dodecyl-OS even at 90% RH. The mass growth factors at 90% RH were determined to be 3.65±0.06, 3.58±0.02 and 1.59±0.01 for methyl-OS, ethyl-OS, and octyl-OS, respectively.

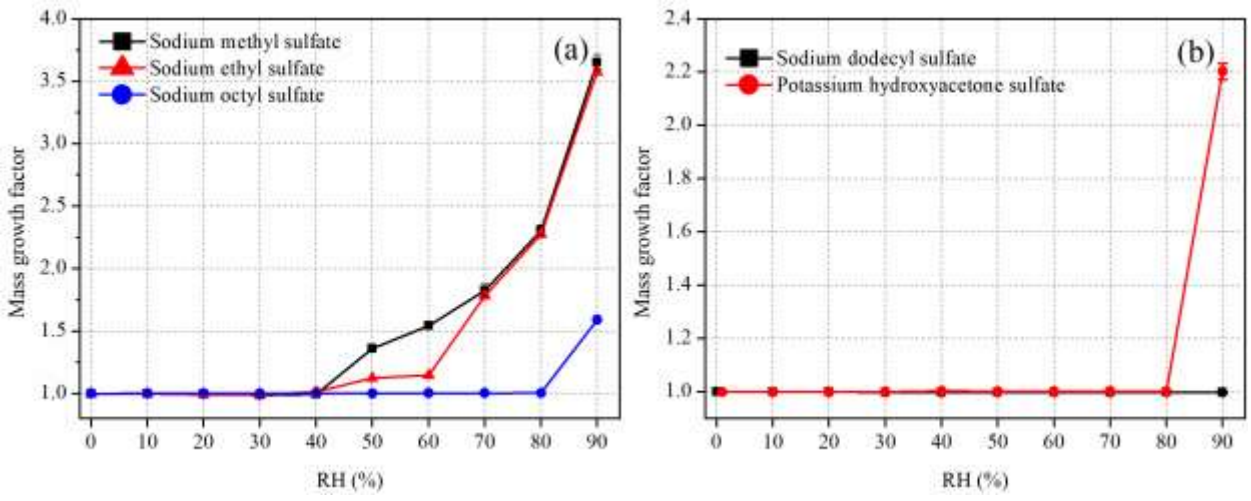

Figure 4. Mass growth factors of (a) methyl-, ethyl- and octyl-OS and (b) dodecyl-OS and potassium hydroxyacetone sulfate as a function of RH at 25 ºC. Please note that error bars are included, but they are too small to be clearly visible.

Mass growth factors of seven potassium organosulfates were also investigated, including potassium hydroxyacetone sulfate, potassium 3-hydroxy phenyl sulfate, potassium benzyl sulfate, potassium 2-methyl benzyl sulfate, potassium 3-methyl benzyl sulfate, potassium 2,4-dimethyl benzyl sulfate and potassium 3,5-dimethyl benzyl sulfate. All the compounds did not show measurable water uptake at 80% RH. When RH was increased to 90%, as shown in Figure 4b, a significant increase in mass was observed for potassium hydroxyacetone sulfate particles, suggesting the occurrence of deliquescence, and the mass growth factor was determined to be 2.20 ±0.03 at 90% RH. No significant water uptake was observed for the other six potassium organosulfates even when RH was increased to 90%. We should mention that occasionally small increase in sample mass (up to 10-20%) was observed for a few samples when RH was increased from 80% to 90%, and such small increase in sample mass may be caused by water uptake of impurities (such as potassium hydroxide) contained in these synthesized compounds.

Table 1. Mass growth factors (m/m_0) and water-to-solute ratios (WSRs) as a function of RH (10-90 %) at 25 ºC for sodium methyl sulfate, sodium ethyl sulfate, sodium octyl sulfate and potassium hydroxyacetone sulfate. All the errors given in this work are standard deviations.

RH (%)	sodium methyl sulfate		sodium ethyl sulfate	
	m/m_0	WSR	m/m_0	WSR
10	1.00 ±0.01	-	1.00 ±0.01	-
20	1.00 ±0.01	-	0.99 ±0.01	-

30	0.99±0.01	-	0.99±0.01	-
40	1.00±0.02	-	1.02±0.03	-
50	1.36±0.02	2.68±0.04	1.13±0.01	-
60	1.55±0.03	4.06±0.09	1.15±0.01	-
70	1.83±0.05	6.16±0.17	1.79±0.02	6.46±0.07
80	2.31±0.04	9.73±0.18	2.27±0.02	10.48±0.11
90	3.65±0.06	19.75±0.34	3.58±0.02	21.19±0.14

RH (%)	sodium octyl sulfate		potassium hydroxyacetone sulfate	
	m/m_0	WSR	m/m_0	WSR
10	1.00±0.01	-	1.00±0.01	-
20	1.00±0.01	-	1.00±0.01	-
30	1.00±0.01	-	1.00±0.01	-
40	1.00±0.01	-	1.00±0.01	-
50	1.00±0.01	-	1.00±0.01	-
60	1.00±0.01	-	1.00±0.01	-
70	1.00±0.01	-	1.00±0.01	-
80	1.01±0.01	-	1.00±0.01	-
90	1.59±0.01	7.63±0.02	2.20±0.03	12.84±0.18

For deliquesced samples, measured mass changes can be converted to water to solute ratios (WSRs), defined as the molar ratio of H_2O to sulfur. The WSRs data are summarized in Table 1 for sodium methyl sulfate, sodium ethyl sulfate, sodium octyl sulfate and potassium hydroxyacetone sulfate. As shown in Table 1, WSRs at 90% RH were determined to be 19.75±0.34, 21.19±0.14, 7.63±0.02 and 12.84±0.18 for sodium methyl sulfate, sodium ethyl sulfate, sodium octyl sulfate and potassium hydroxyacetone sulfate at 25 °C.

3.2 Hygroscopic growth of aerosols

3.2.1 Organosulfates

H-TDMA was employed to measure hygroscopic growth factors of 100 nm methyl-, ethyl- and octyl-OS aerosols as a function of RH (up to 90%), and the results are shown in Figure 5 and Table 2. In addition, no significant hygroscopic growth was observed for dodecyl-OS for RH up to 90%. We did not investigate hygroscopic growth of other OS aerosols due to the very small quantity of these synthesized compounds.

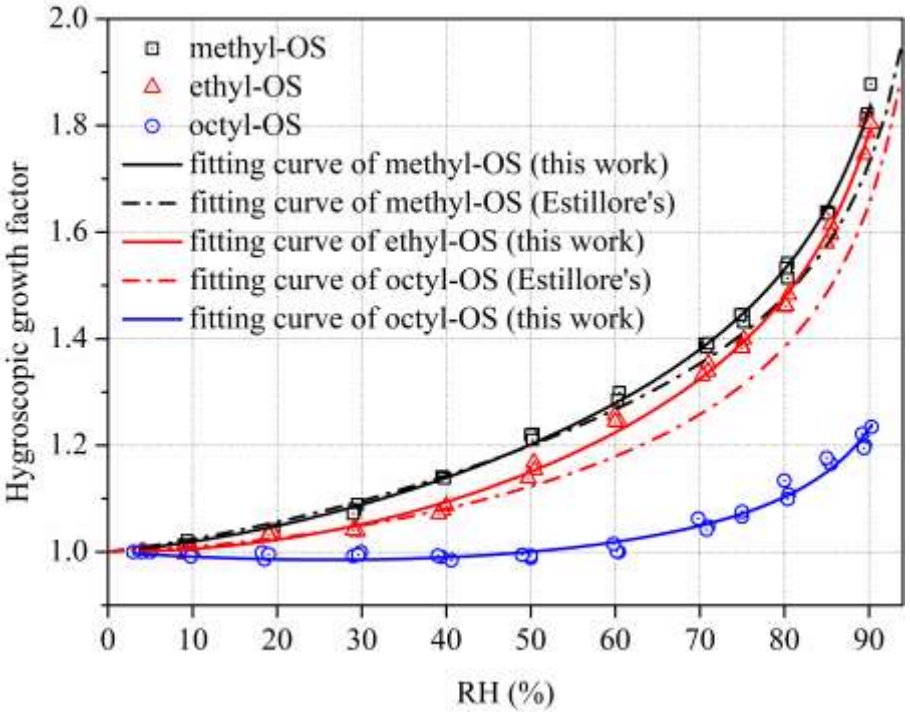

Figure 5. Hygroscopic growth factors of (a) methyl- and octyl-OS and (b) ethyl-OS aerosols as a function of RH. Solid curves represent fitted curves in our work using Eq. (1). For comparison, the fitted curves reported by Estillore et al. (2016) are presented by dashed curves.

As shown in Figure 5, methyl-, ethyl- and octyl-OS aerosols all exhibited continuous hygroscopic growth without obvious phase transitions. To our knowledge, only one previous study

(Estillore et al., 2016) investigated hygroscopic growth of methyl- and ethyl-OS aerosols using a H-TDMA, and continuous hygroscopic growth was also observed. The continuous growth behavior can be attributed to the amorphous state of aerosol particles, which would take up water at very low RH. For methyl-OS aerosol, GFs were determined in our work to be 1.53±0.01, 1.63±0.01 and 1.83±0.03 at 80%, 85% and 90% RH; for comparison, its GF was measured to be 1.50 at 85% RH by Estillore et al. (2016), only ~8% smaller than our result. In our work, GFs were determined to be 1.47±0.01, 1.60±0.02 and 1.79±0.02 at 80%, 85% and 90% RH for ethyl-OS aerosol; for comparison, it was measured to be 1.45 at 85% RH in the previous study (Estillore et al., 2016), only ~9% smaller than our result. As DMA sizing typically has a relative uncertainty of 5-7% (Wiedensohler et al., 2012), our measured GFs agree very well with those reported by Estillore et al. (2016) for methyl- and ethyl-OS, while the highest RH we reached was 90%, compared to 85% by Estillore et al. (2016). With respect to octyl-OS aerosol, GF were determined to be 1.11±0.02, 1.17±0.01 and 1.21±0.02 at 80%, 85% and 90% RH in our work; to our knowledge, hygroscopic growth of octyl-OS aerosol has not been explored previously. Compared to ammonium sulfate (1.75 at 90% RH), GFs at 90% RHs were found to be slightly larger for methyl- and ethyl-OS, but significantly smaller for octyl-OS.

Table 2. Hygroscopic growth factors (GFs) of methyl-, ethyl- and octyl-OS aerosols at different RH. All the errors given in this work are standard deviations.

RH (%)	sodium methyl sulfate	sodium ethyl sulfate	sodium octyl sulfate
5	1.00±0.01	1.00±0.01	1.00±0.01
10	1.01±0.01	1.00±0.01	1.00±0.01
20	1.04±0.01	1.03±0.01	0.99±0.01
30	1.08±0.01	1.04±0.01	1.00±0.01

40	1.14±0.01	1.08±0.01	0.99±0.01
50	1.22±0.01	1.15±0.01	0.99±0.01
60	1.29±0.01	1.25±0.01	1.01±0.01
70	1.39±0.01	1.34±0.01	1.05±0.01
75	1.44±0.01	1.39±0.01	1.07±0.01
80	1.53±0.01	1.47±0.01	1.11±0.02
85	1.63±0.01	1.60±0.02	1.17±0.01
90	1.83±0.03	1.79±0.02	1.21±0.02

When aerosol particles take up water continuously, the RH-dependent GFs can usually be fitted using Eq. (1) (Kreidenweis et al., 2005):

$$\mathrm{GF} = [1 + (a + b \cdot \frac{\mathrm{RH}}{100} + c \cdot (\frac{\mathrm{RH}}{100})^2) \cdot \frac{\mathrm{RH}}{100-\mathrm{RH}}]^{1/3} \qquad (1)$$

where *a*, *b* and *c* are coefficients obtained from fitting using Eq. (1). As shown in Figure 5, hygroscopic growth factors of methyl-, ethyl- and octyl-OS aerosols can be fitted by Eq. (1), and the obtained coefficients (*a*, *b* and *c*) are summarized in Table 3.

Table 3. The three coefficients (*a*, *b* and *c*) obtained by using Eq. (1) to fit RH-dependent GFs for sodium methyl sulfate, sodium ethyl sulfate and sodium octyl sulfate aerosols.

organosulfates	*a*	*b*	*c*
sodium methyl sulfate	0.42182	1.20336	-1.15508
sodium ethyl sulfate	0.00174	1.61805	-1.15502
sodium octyl sulfate	-0.31868	0.86233	-0.44623

3.2.2 Comparison between VSA and H-TDMA measurements

Figure 4 shows that obvious deliquescence transitions were observed for methyl-, ethyl-, and octyl-OS in the VSA experiments, because samples used in VSA experiments may be crystalline salts; in contrast, as revealed by Figure 5, continuous hygroscopic growth without obvious phase transitions was observed for methyl-, ethyl- and octyl-OS aerosol particles in H-TDMA measurements, suggesting that these aerosol particles which were produced by drying aqueous droplets to <5% RH may exist in amorphous state. Estillore et al. (2016) employed a H-TDMA to investigate hygroscopic properties of several OS aerosols, and similarly they found that those aerosols, including methyl-OS, ethyl-OS and potassium hydroxyacetone sulfate which were also examined in our work, displayed continuous hygroscopic growth.

For completely deliquesced particles, if it is assumed that the particle is spherical and that the particle volume at a given RH is equal to the sum of the dry particle volume and the volume of particulate water, particle mass change, measured using the VSA, can then be converted to hygroscopic GF, using Eq. (2):

$$\mathrm{GF} = \sqrt[3]{1 + (\frac{m}{m_0} - 1) \cdot \frac{\rho_0}{\rho_w}} \quad (2)$$

where ρ_0 and ρ_w are the density of the dry sample and water, respectively. The density of methyl-, ethyl- and octyl-OS particles were reported to be 1.60, 1.46 and 1.19 g cm^{-3} with an uncertainty of 20-30% (Kwong et al., 2018; ChemistryDashboard, 2021). Figure 6 compares VSA-derived GFs and those measured using H-TDMA for methyl-, ethyl- and octyl-OS, and it can be concluded that for RH at which samples used in the VSA experiments were deliquesced, GFs derived from mass change measured using VSA agree relatively well with those directly measured using H-TDMA. For example, at 90% RH GFs were measured by H-TDMA to be 1.83±0.03, 1.79±0.02 and 1.21±0.02 for methyl-, ethyl- and octyl-OS, while at the same RH their GFs derived from VSA

measurements were found to be 1.74±0.01, 1.68±0.01 and 1.19±0.01, only 6% (or less) smaller than those measured using H-TDMA. The small but systematical differences between VSA and H-TDMA results, as evident from Figure 6, could stem from volume additivity assumption used to convert mass growth to diameter growth, uncertainties in OS densities, and DMA sizing errors.

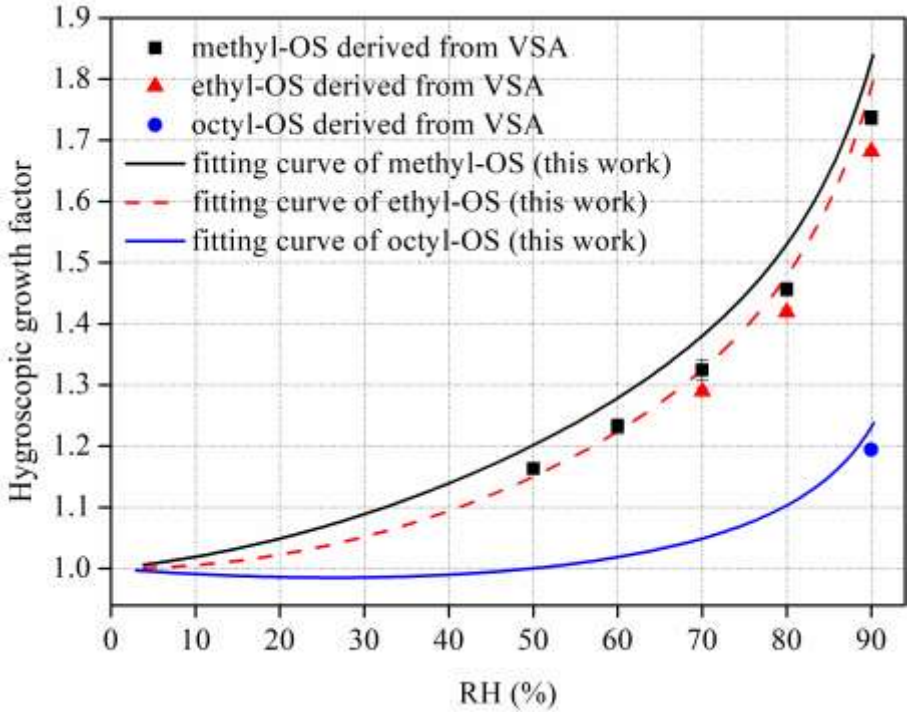

Figure 6. Comparison between hygroscopic GFs of methyl-, ethyl- and octyl-OS derived from VSA experiments to those measured using H-TDMA. Please note that H-TDMA results are presented as the three-parameter curves obtained. Error bars are included, but they are too small to be clearly visible.

3.2.3 Internally mixed aerosols

We also investigated hygroscopic properties of methyl-, ethyl- and octyl-OS aerosols internally mixed with ammonium sulfate (AS), and the results are summarized in Table 4. Figure 7a displays GFs of 100 nm methyl-OS/AS mixed aerosols with mass ratios of 1:1 and 1:5. The 1:1

316 mixed aerosol particle showed a deliquescence transition at 70% RH, while the 1:5 mixed aerosols
317 showed a deliquescence transition at 75% RH, which was lower than the deliquescence RH (DRH,
318 80%) of AS. Here the DRH is defined as the RH at which the mixed aerosols are completely
319 deliquesced (Choi and Chan, 2002). Figure 7a suggests that before full deliquescence, significant
320 hygroscopic growth was also observed, i.e. pre-deliquescence of mixed particles occurred when
321 RH was lower than their DRH. Pre-deliquescence was widely reported in previous studies which
322 investigated hygroscopic properties of inorganic/organic mixed aerosols (Choi and Chan, 2002;
323 Prenni, 2003; Wise et al., 2003; Brooks, 2004; Marcolli and Krieger, 2006; Wu et al., 2011; Lei et
324 al., 2014; Jing et al., 2016; Estillore et al., 2017). For example, Choi and Chan. (2002) investigated
325 hygroscopic behaviors of internal mixed particles which consisted of water-soluble organic
326 compounds and AS, and found that the internal mixing with organics (such as malonic and citric
327 acids) could reduce the DRH of AS, due to the ability of organics to absorb water at low RH.

328 Internal mixing with ethyl- and octyl-OS could also reduce the DRH of AS. As shown in
329 Figure 7b, ethyl-OS/AS mixed aerosols were deliquesced at 70% RH when the mass ratio of ethyl-
330 OS to AS was 1:1 and at 80% RH when the mass ratio was 1:5. In addition, Figure 7c suggested
331 that the deliquescence of octyl-OS/AS aerosols took place at 75% RH for the 1:1 mixture and at
332 80% for 1:5 mixture.

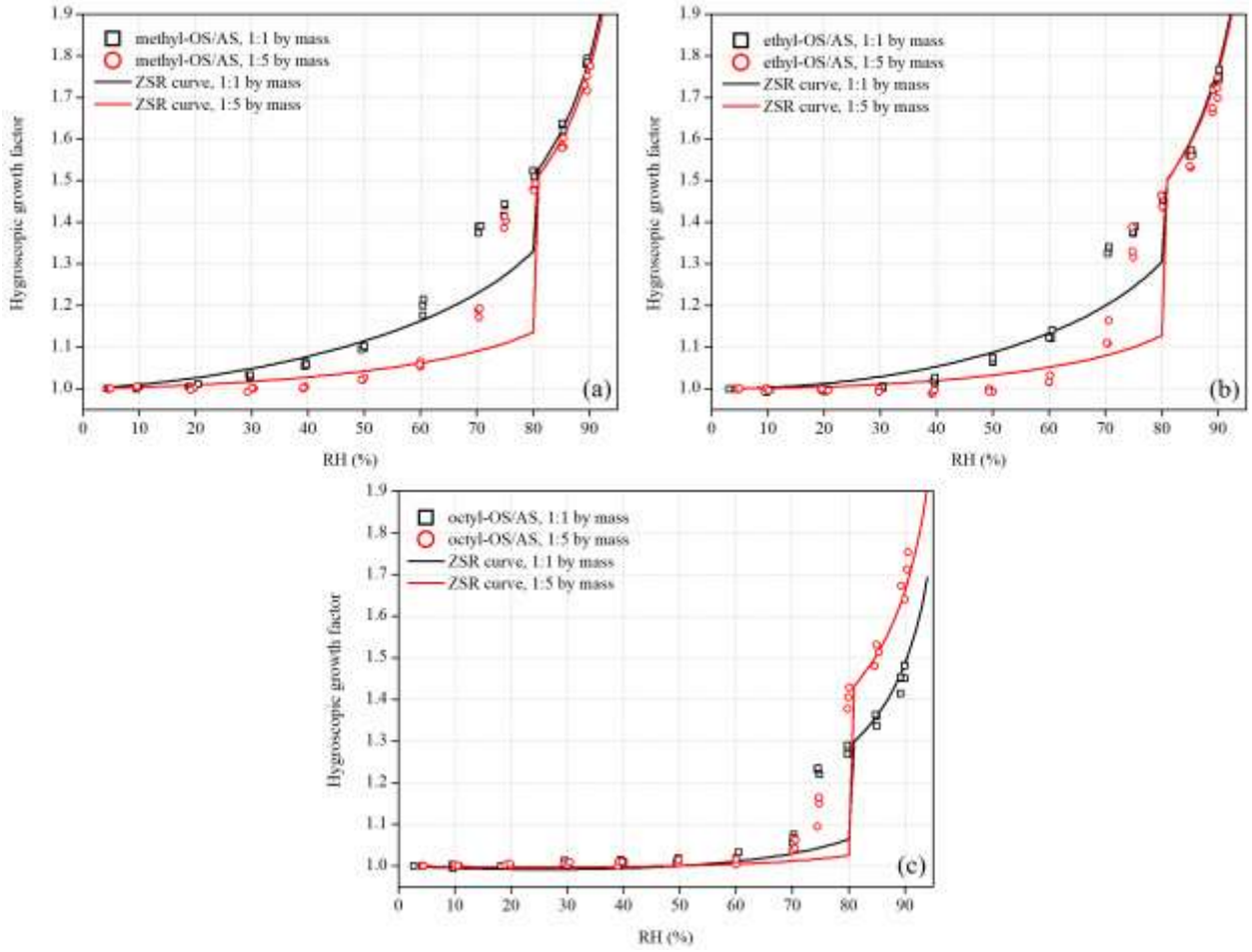

333

334 **Figure 7.** Hygroscopic growth factors of (a) methyl-OS/AS, (b) ethyl-OS/AS, and (c) octyl-OS/AS
335 aerosols as a function of RH. The mass ratios of methyl-, ethyl-, and octyl-OS to AS were 1:1 and
336 1:5, respectively. Solid curves represent hygroscopic growth factors of mixed aerosols predicted
337 using the ZSR method.

338

339 **Table 4.** Hygroscopic GF of methyl-, ethyl, and octyl-OS internally mixed with AS (their mass
340 ratios are 1:1 and 1:5) at different RH. All the errors given in this work are standard deviations.

RH (%)	methyl-OS/AS		ethyl-OS/AS		octyl-OS/AS	
	1:1	1:5	1:1	1:5	1:1	1:5
5	1.00±0.01	1.00±0.01	1.00±0.01	1.00±0.01	1.00±0.01	1.00±0.01
10	1.00±0.01	1.00±0.01	1.00±0.01	1.00±0.01	1.00±0.01	1.00±0.01

20	1.01±0.01	1.00±0.01	1.00±0.01	1.00±0.01	1.00±0.01	1.00±0.01
30	1.03±0.01	1.00±0.01	1.00±0.01	1.00±0.01	1.01±0.01	1.01±0.01
40	1.06±0.01	1.00±0.01	1.02±0.01	0.99±0.01	1.01±0.01	1.01±0.01
50	1.10±0.01	1.02±0.01	1.07±0.01	0.99±0.01	1.01±0.01	1.01±0.01
60	1.20±0.02	1.06±0.01	1.13±0.01	1.02±0.01	1.02±0.01	1.01±0.01
70	1.38±0.01	1.19±0.01	1.33±0.01	1.13±0.03	1.07±0.01	1.05±0.01
75	1.43±0.01	1.40±0.01	1.38±0.01	1.34±0.04	1.23±0.01	1.14±0.03
80	1.52±0.01	1.48±0.01	1.46±0.01	1.45±0.02	1.28±0.01	1.40±0.02
85	1.63±0.01	1.59±0.01	1.56±0.01	1.54±0.02	1.35±0.02	1.51±0.02
90	1.79±0.01	1.74±0.02	1.74±0.02	1.72±0.02	1.47±0.02	1.69±0.04

The Zdanovskii-Stokes-Robinson (ZSR) method (Stokes and Robinson, 1966) has been widely used to predict hygroscopic growth of internally mixed aerosol particles, assuming that the interaction among individual species are negligible and that individual species in the mixed particles take up water independently. According to the ZSR method, GF of a mixed particle, GF_{mix}, can be calculated using Eq. (3) (Malm and Kreidenweis, 1997):

$$\mathrm{GF_{mix}} = \sqrt[3]{\sum(\varepsilon_i \cdot \mathrm{GF}_i^3)} \quad (3)$$

where GF_i is the GF of *i*th species the dry mixed particle contains. The volume fraction of the *i*th species in the dry mixed particle, ε_i, can be calculated using Eq. (4):

$$\varepsilon_i = \frac{m_i/\rho_i}{\sum(m_i/\rho_i)} \quad (4)$$

where m_i and ρ_i are the mass fraction and density of the *i*th species. GFs of pure OS, measured in our work using H-TDMA and presented in Section 3.2.1, and GFs of AS, calculated using the E-AIM model (Clegg et al., 1998; Wexler and Clegg, 2002), were used as input to predict GFs of methyl-, ethyl- and octyl-OS internally mixed with AS. Comparisons between measured and predicted GFs are displayed in Figure 7 for OS/AS mixed aerosols.

As shown in Figure 7a, GFs of methyl-OS/AS mixed aerosols (both the 1:1 and 1:5 mixtures) could be well predicted using the ZSR method when RH was <60% or >80%, while the ZSR method underestimated their GFs at 70% and 75% RH. Such underestimation at 70% and 75% RH is likely to due to that inorganic compounds (AS, in our work) may dissolve partially in the organics/water solution (which can be formed at much lower RH due to continuous water uptake of organics) before the mixed particle is completely deliquesced (Svenningsson et al., 2006; Zardini et al., 2008; Wu et al., 2011); in contrast, the ZSR method assumes that individual species take up water independently. As shown in Figure 7, the ZSR method also underestimated GFs at 70 and 75% RH for ethyl-OS/AS and octyl-OS/AS mixed aerosols, though good agreement between measurement and prediction was found at other RH. For example, the ratios of partially dissolved AS to total AS at 70% RH were estimated to be 0.95, 0.85 and 0.49 for methyl-OS/AS, ethyl-OS/AS, and octyl-OS/AS mixtures with a mass ratio of 1:1.

3.3 Cloud condensation nucleation activities

Figures 3, S2 and S3 show CCN activation curves obtained at four supersaturations for methyl-, ethyl- and octyl-OS aerosols and their internal mixtures with ammonium sulfate. Each activation curve was fitted using a Boltzmann sigmoid function to derive the corresponding critical particle diameter (d_{50}), which was then used to calculate κ_{ccn} using Eqs. (5a-5b) (Petters and Kreidenweis, 2007):

$$\kappa_{\mathrm{ccn}} = \frac{4A^3}{27 d_{50}^3 \ln^2 S_c} \quad (5a)$$

$$A = \frac{4\sigma_{s/a} M_w}{RT\rho_w} \quad (5b)$$

where S_c is the critical saturation ratio (1+SS) of water; d_{50} is the critical particle diameter; A is a constant which describes the Kelvin effect on a curved surface of a droplet, and depends on the surface tension ($\sigma_{s/a}$), molecular weight (M_w), density (ρ_w) of water, temperature (T) and the

379 universal gas constant (R). Table 5 summarizes critical diameters at different supersaturations for
380 aerosol particles examined in this work and their κ_{ccn} values.

381

382 **Table 5.** Single hygroscopicity parameters derived from hygroscopic growth (κ_{gf}) and CCN
383 activity measurements (κ_{ccn}) for methyl-, ethyl- and octyl-OS and their internal mixtures with
384 ammonium sulfate (AS). All errors given were standard deviations.

aerosol	mass ratio	*SS* (%)	d_{50} (nm)	κ_{ccn}	average κ_{ccn}	κ_{gf}
methyl-OS	-	0.45	52.9 ±0.9	0.432-0.477	0.459 ±0.021	0.537-0.604
	-	0.67	41.1 ±0.8	0.416-0.468		
	-	0.87	33.3 ±0.4	0.471-0.507		
	-	1.13	28.8 ±0.5	0.431-0.477		
methyl-OS/AS	1:5	0.45	51.9 ±0.5	0.467-0.492	0.453 ±0.027	0.454-0.495
	1:5	0.67	41.6 ±0.4	0.411-0.436		
	1:5	0.87	33.7 ±0.5	0.453-0.490		
	1:5	1.13	29.2 ±0.6	0.412-0.464		
ethyl-OS	-	0.45	55.5 ±0.8	0.375-0.410	0.397 ±0.010	0.505-0.548
	-	0.67	42.8 ±0.6	0.376-0.406		
	-	0.87	35.3 ±0.5	0.395-0.428		
	-	1.13	30.2 ±0.3	0.382-0.408		
ethyl-OS/AS	1:5	0.45	52.3 ±1.2	0.437-0.504	0.458 ±0.024	0.435-0.474
	1:5	0.67	41.0 ±0.5	0.426-0.459		
	1:5	0.87	33.4 ±0.6	0.463-0.512		
	1:5	1.13	29.2 ±0.6	0.409-0.462		
octyl-OS	-	0.45	70.0 ±1.2	0.186-0.207	0.206 ±0.008	0.076-0.096
	-	0.67	53.2 ±0.6	0.196-0.211		
	-	0.87	44.1 ±0.7	0.202-0.221		
	-	1.13	37.1 ±0.8	0.200-0.227		
octyl-OS/AS	1:5	0.45	53.7 ±0.9	0.413-0.456	0.436 ±0.009	0.388-0.464
	1:5	0.67	41.1 ±0.5	0.426-0.458		
	1:5	0.87	34.4 ±0.5	0.427-0.462		

1:5	1.13	29.5±0.2	0.413-0.434

As shown in Table 5, κ_{ccn} values were determined to be 0.459±0.021, 0.397±0.010 and 0.206±0.008 for methyl-, ethyl- and octyl-OS, decreasing with alkyl chain length, and this suggests that the addition of hydrophobic hydrocarbon functional groups to OS reduced their hygroscopicity. Decrease in hygroscopicity of OS compounds with the increase in the number of carbon atoms was also observed under subsaturated conditions (Section 3.2). In addition, we investigated CCN activities of alkyl-OS/AS mixed aerosols with a mass ratio of 1:5, and κ_{ccn} values were determined to be 0.453±0.027, 0.458±0.024 and 0.436±0.009 for methyl-OS/AS, ethyl-OS/AS and octyl-OS/AS.

3.3.1 Comparison between H-TDMA and CCN activities measurements

It is suggested that the single hygroscopicity parameter, κ, could describe aerosol-water interactions under both sub- and supersaturated conditions (Petters and Kreidenweis, 2007). The κ values derived from CCN activity measurements, κ_{ccn}, have been illustrated above; the κ values derived from H-TDMA measurements, κ_{gf}, can be calculated using Eq. (6) (Petters and Kreidenweis, 2007; Tang et al., 2016):

$$\kappa_{gf} = (GF^3 - 1)\frac{1-RH}{RH} \quad (6)$$

In this work GF measured at 90% RH were used to calculate κ_{gf} values, which are also listed in Table 5. Eq. (6) does not take into account the Kelvin effect as the effect is small for 100 nm particles (Tang et al., 2016).

Figure 8 compares κ_{ccn} and κ_{gf} values for the six types of aerosol particles examined. For pure OS, κ_{ccn} of methyl-OS (0.459±0.021) and ethyl-OS (0.397±0.010) were smaller than their κ_{gf} values (0.537-0.604 and 0.505-0.548), but the relative differences do not exceed 25%. Such a

difference (<25%) may not be significant if all the uncertainties associated with deriving κ from measured hygroscopic growth and CCN activities (Petters and Kreidenweis, 2007). Octyl-OS appears to be an exception, and the average κ_{ccn} (0.206) was ~2.4 times larger than the average κ_{gf} (0.086). In addition, no significant difference was observed between κ_{ccn} and κ_{gf} for all the alkyl-OS/AS mixed aerosols.

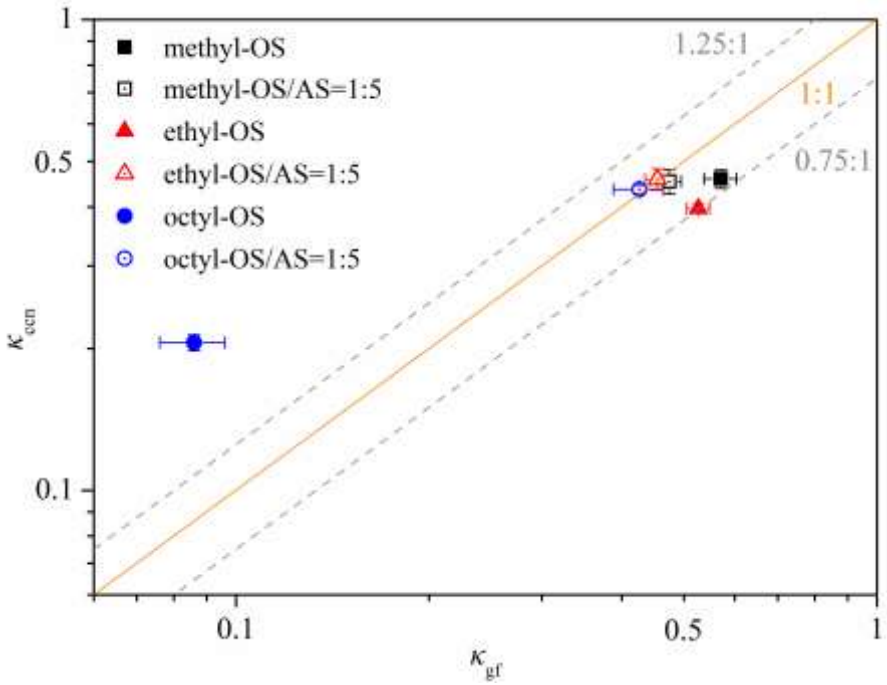

Figure 8. Comparison of κ values derived from hygroscopic growth (κ_{gf}) with these derived from CCN activities (κ_{ccn}) for methyl-, ethyl- and octyl-OS aerosols as well as their internal mixtures with ammonium sulfate (the mass ratio was 1:5).

Significant differences between κ_{gf} and κ_{ccn} were reported in previous studies (Petters et al., 2009; Wex et al., 2009; Hansen et al., 2015), attributed to several factors discussed below. Petters and Kreidenweis. (2008) demonstrated that cloud droplet activation was highly sensitive to the solubility for sparingly soluble compounds in the range of 5×10^{-4}-2×10^{-1}, expressed as volume of

solute per unit volume of water (Petters and Kreidenweis, 2008). Compared to the highly soluble methyl- and ethyl-OS (their solubilities are 0.127-0.219 and 0.075-0.151), the solubility of octyl-OS (8.43×10^{-4}-4.26×10^{-2}) (Chemistry Dashboard, 2021) is rather limited, and incomplete dissolution at subsaturated condition in H-TDMA measurements may lead to underestimation of κ_{gf} values for octyl-OS; as a result, the solubility limit may explain the observed difference between κ_{gf} and κ_{ccn} for octyl-OS. Furthermore, surface tension is a key factor to influence critical supersaturations at which aerosol particles are activated to cloud droplets (Petters and Kreidenweis, 2013). We measured surface tensions of alkyl-OS and alkyl-OS/AS (the mass ratio was 1:5) solutions, and the results are shown in Table S1 and Figure S4. The surface tension of octyl-OS is much lower than that of pure water, leading to significant reduction in critical supersaturations and thus overestimation of its κ_{ccn} value; for comparison, the surface tension depression is also visible but much less pronounced for octyl-OS/AS mixed aerosol. Overall, we proposed that solubility limit and surface tension reduction may both contribute to the observed discrepancy between κ_{gf} and κ_{ccn} values for octyl-OS aerosol. We note that some numerical models (Petters and Kreidenweis, 2008, 2013; Riipinen et al., 2015) are available to quantitatively assess contribution of solubility limit and surface tension reduction to the discrepancy between κ_{gf} and κ_{ccn}.

4. Conclusions

Organosulfates (OS) may contribute significantly to secondary organic aerosols in various locations over the globe; however, their hygroscopic properties and CCN activities have not been well understood. In this work, three complementary techniques, including a vapor sorption analyzer (VSA), a hygroscopicity tandem differential mobility analyzer (H-TDMA) and a cloud condensation nuclei counter (CCNc), were employed to investigate interactions of several OS with

water vapor under sub- and supersaturated conditions, trying to get a comprehensive picture of their hygroscopic properties and CCN activities.

VSA was used to measure mass change of OS samples with RH (0-90%). Obvious deliquescence was found for sodium methyl sulfate (methyl-OS), sodium ethyl sulfate (ethyl-OS), sodium octyl sulfate (octyl-OS) and potassium hydroxyacetone sulfate, and their mass growth factors at 90% RH were determined to be 3.65 ±0.06, 3.58 ±0.02, 1.59 ±0.01 and 2.20 ±0.03, respectively. No significant water uptake were observed up to 90% RH for other OS compounds examined, including sodium dodecyl sulfate, potassium 3-hydroxy phenyl sulfate, potassium benzyl sulfate, potassium 2-methyl benzyl sulfate, potassium 3-methyl benzyl sulfate, potassium 2,4-dimethyl benzyl sulfate and potassium 3,5-dimethyl benzyl sulfate. Hygroscopic properties of methyl-, ethyl- and octyl-OS aerosols were also studied using H-TDMA, which measured mobility diameters of aerosol particles as a function of RH. Continuous hygroscopic growth was observed for methyl-, ethyl- and octyl-OS aerosols, and their growth factors at 90% RH were measured to be 1.83 ±0.03, 1.79 ±0.02 and 1.21 ±0.02.

We further investigated CCN activities of methyl-, ethyl- and octyl-OS aerosols, and their single hygroscopicity parameters, κ_{ccn}, were determined to be 0.459 ±0.021, 0.397 ±0.010 and 0.206 ±0.008, respectively. For methyl- and ethyl-OS aerosols, single hygroscopicity parameters derived from CCN activities (κ_{ccn}) agree reasonably well with those derived from H-TDMA measurements (κ_{gf}) with relative differences being <25%. However, κ_{ccn} was found to be ~2.4 times larger than κ_{gf} for octyl-OS, and we show that solubility limit and surface tension reduction may both contribute to such discrepancy observed.

Data availability. Data used in this paper can be found in the main text or supplement.

Competing interests. The authors declare that they have no conflict of interest.

Author contribution. Mingjin Tang conceived this work; Ru-Jin Huang, Yuqing Zhang, Xiang Ding and Xinming Wang chose and provided samples investigated in this work; Chao Peng, Lanxiadi Chen, Yuqing Zhang and Xiang Ding conducted VSA measurements; Chao Peng, Weigang Wang and Maofa Ge conducted H-TDMA measurements; Patricia N. Razafindrambinina, Kotiba A. Malek and Akua A. Asa-Awuku conducted CCN activity measurements; Chao Peng, Patricia N. Razafindrambinina, Kotiba A. Malek, Akua A. Asa-Awuku and Mingjin Tang analyzed the data and prepared the manuscript with contribution from all the other coauthors.

Financial support

This work was funded by National Natural Science Foundation of China (91744204), China Postdoctoral Science Foundation (2020M682931), Ministry of Science and Technology of China (2018YFC0213901), State Key Laboratory of Loess and Quaternary Geology (SKLLQG1921), Guangdong Foundation for Program of Science and Technology Research (2017B030314057, 2019B121205006 and 2020B1212060053), Guangdong Science and Technology Department (2017GC010501) and CAS Pioneer Hundred Talents program.

References

Brooks, S.: Water uptake by particles containing humic materials and mixtures of humic materials with ammonium sulfate, Atmos. Environ., 38, 1859-1868, 2004.

Bruggemann, M., Xu, R., Tilgner, A., Kwong, K. C., Mutzel, A., Poon, H. Y., Otto, T., Schaefer, T., Poulain, L., Chan, M. N., and Herrmann, H.: Organosulfates in Ambient Aerosol: State of Knowledge and Future Research Directions on Formation, Abundance, Fate, and Importance, Environmental science & technology, 2020.

ChemistryDashboard: United States Environmental Protection Agency, available at: https://comptox.epa.gov/dashboard, last access: 12 January 2021, in, 2021.

Chen, L., Chen, Y., Chen, L., Gu, W., Peng, C., Luo, S., Song, W., Wang, Z., and Tang, M.: Hygroscopic Properties of 11 Pollen Species in China, ACS Earth and Space Chemistry, 3, 2678-2683, 2019.

Choi, M. Y., and Chan, C. K.: The effects of organic species on the hygroscopic behaviors of inorganic aerosols, Environmental Science & Technology, 36, 2422-2428, 2002.

Clegg, S. L., and Brimblecombe, P.: Equilibrium partial pressures of strong acids over concentrated saline solutions-1. HNO3, Atmospheric Environment, 22, 91-100, 1988.

Clegg, S. L., Brimblecombe, P., and Wexler, A. S.: Thermodynamic model of the system H+-NH4+-Na+-SO42--NB3--Cl--H2O at 298.15 K, J. Phys. Chem. A, 102, 2155-2171, 1998.

Ervens, B., Turpin, B., and Weber, R.: Secondary organic aerosol formation in cloud droplets and aqueous particles (aqSOA): a review of laboratory, field and model studies, Atmospheric Chemistry and Physics, 11, 11069-11102, 2011.

Estillore, A. D., Hettiyadura, A. P. S., Qin, Z., Leckrone, E., Wombacher, B., Humphry, T., Stone, E. A., and Grassian, V. H.: Water Uptake and Hygroscopic Growth of Organosulfate Aerosol, Environmental Science & Technology, 50, 4259-4268, 2016.

Estillore, A. D., Morris, H. S., Or, V. W., Lee, H. D., Alves, M. R., Marciano, M. A., Laskina, O., Qin, Z., Tivanski, A. V., and Grassian, V. H.: Linking hygroscopicity and the surface microstructure of model inorganic salts, simple and complex carbohydrates, and authentic sea spray aerosol particles, Physical Chemistry Chemical Physics, 19, 21101-21111, 2017.

Froyd, K. D., Murphy, S. M., Murphy, D. M., de Gouw, J. A., Eddingsaas, N. C., and Wennberg, P. O.: Contribution of isoprene-derived organosulfates to free tropospheric aerosol mass, Proceedings of the National Academy of Sciences of the United States of America, 107, 21360-21365, 2010.

Gu, W., Li, Y., Zhu, J., Jia, X., Lin, Q., Zhang, G., Ding, X., Song, W., Bi, X., Wang, X., and Tang, M.: Investigation of water adsorption and hygroscopicity of atmospherically relevant particles using a commercial vapor sorption analyzer, Atmospheric Measurement Techniques, 10, 3821-3832, 2017.

Guo, L., Gu, W., Peng, C., Wang, W., Li, Y. J., Zong, T., Tang, Y., Wu, Z., Lin, Q., Ge, M., Zhang, G., Hu, M., Bi, X., Wang, X., and Tang, M.: A comprehensive study of hygroscopic properties of calcium- and magnesium-containing salts: implication for hygroscopicity of mineral dust and sea salt aerosols, Atmospheric Chemistry and Physics, 19, 2115-2133, 2019.

Hallquist, M., Wenger, J. C., Baltensperger, U., Rudich, Y., Simpson, D., Claeys, M., Dommen, J., Donahue, N. M., George, C., Goldstein, A. H., Hamilton, J. F., Herrmann, H., Hoffmann, T., Iinuma, Y., Jang, M., Jenkin, M. E., Jimenez, J. L., Kiendler-Scharr, A., Maenhaut, W., McFiggans, G., Mentel, T. F., Monod, A., Prevot, A. S. H., Seinfeld, J. H., Surratt, J. D., Szmigielski, R., and Wildt, J.: The formation, properties and impact of secondary organic aerosol: current and emerging issues, Atmospheric Chemistry And Physics, 9, 5155-5236, 2009.

Hansen, A. M. K., Kristensen, K., Nguyen, Q. T., Zare, A., Cozzi, F., Nojgaard, J. K., Skov, H., Brandt, J., Christensen, J. H., Strom, J., Tunved, P., Krejci, R., and Glasius, M.: Organosulfates and organic acids in Arctic aerosols: speciation, annual variation and concentration levels, Atmospheric Chemistry and Physics, 14, 7807-7823, 2014.

Hansen, A. M. K., Hong, J., Raatikainen, T., Kristensen, K., Ylisirnio, A., Virtanen, A., Petaja, T., Glasius, M., and Prisle, N. L.: Hygroscopic properties and cloud condensation nuclei activation of limonene-derived organosulfates and their mixtures with ammonium sulfate, Atmospheric Chemistry and Physics, 15, 14071-14089, 2015.

He, Q.-F., Ding, X., Wang, X.-M., Yu, J.-Z., Fu, X.-X., Liu, T.-Y., Zhang, Z., Xue, J., Chen, D.-H., Zhong, L.-J., and Donahue, N. M.: Organosulfates from Pinene and Isoprene over the Pearl River Delta, South China: Seasonal Variation and Implication in Formation Mechanisms, Environmental Science & Technology, 48, 9236-9245, 2014.

Heald, C. L., Jacob, D. J., Park, R. J., Russell, L. M., Huebert, B. J., Seinfeld, J. H., Liao, H., and Weber, R. J.: A large organic aerosol source in the free troposphere missing from current models, Geophysical Research Letters, 32, 2005.

Hettiyadura, A. P. S., Stone, E. A., Kundu, S., Baker, Z., Geddes, E., Richards, K., and Humphry, T.: Determination of atmospheric organosulfates using HILIC chromatography with MS detection, Atmospheric Measurement Techniques, 8, 2347-2358, 2015.

Hettiyadura, A. P. S., Jayarathne, T., Baumann, K., Goldstein, A. H., de Gouw, J. A., Koss, A., Keutsch, F. N., Skog, K., and Stone, E. A.: Qualitative and quantitative analysis of atmospheric organosulfates in Centreville, Alabama, Atmospheric Chemistry and Physics, 17, 1343-1359, 2017.

Huang, R.-J., Cao, J., Chen, Y., Yang, L., Shen, J., You, Q., Wang, K., Lin, C., Xu, W., Gao, B., Li, Y., Chen, Q., Hoffmann, T., O'Dowd, C. D., Bilde, M., and Glasius, M.: Organosulfates in atmospheric aerosol: synthesis and quantitative analysis of PM2.5 from Xi'an, northwestern China, Atmospheric Measurement Techniques, 11, 3447-3456, 2018.

Hughes, D. D., and Stone, E. A.: Organosulfates in the Midwestern United States: abundance, composition and stability, Environmental Chemistry, 16, 312-322, 2019.

Jimenez, J., Canagaratna, M., Donahue, N., Prevot, A., Zhang, Q., Kroll, J. H., DeCarlo, P. F., Allan, J. D., Coe, H., and Ng, N.: Evolution of organic aerosols in the atmosphere, Science, 326, 1525-1529, 2009.

Jing, B., Tong, S., Liu, Q., Li, K., Wang, W., Zhang, Y., and Ge, M.: Hygroscopic behavior of multicomponent organic aerosols and their internal mixtures with ammonium sulfate, Atmospheric Chemistry and Physics, 16, 4101-4118, 2016.

552 Kanakidou, M., Seinfeld, J., Pandis, S., Barnes, I., Dentener, F., Facchini, M., Dingenen, R. V., Ervens, B., Nenes, A.,
553 and Nielsen, C.: Organic aerosol and global climate modelling: a review, Atmospheric Chemistry and Physics, 5,
554 1053-1123, 2005.
555 Kreidenweis, S. M., Koehler, K., DeMott, P. J., Prenni, A. J., Carrico, C., and Ervens, B.: Water activity and activation
556 diameters from hygroscopicity data - Part I: Theory and application to inorganic salts, Atmospheric Chemistry and
557 Physics, 5, 1357-1370, 2005.
558 Kristensen, K., and Glasius, M.: Organosulfates and oxidation products from biogenic hydrocarbons in fine aerosols
559 from a forest in North West Europe during spring, Atmospheric Environment, 45, 4546-4556, 2011.
560 Kundu, S., Quraishi, T. A., Yu, G., Suarez, C., Keutsch, F. N., and Stone, E. A.: Evidence and quantitation of aromatic
561 organosulfates in ambient aerosols in Lahore, Pakistan, Atmospheric Chemistry and Physics, 13, 4865-4875, 2013.
562 Kwong, K. C., Chim, M. M., Davies, J. F., Wilson, K. R., and Chan, M. N.: Importance of sulfate radical anion
563 formation and chemistry in heterogeneous OH oxidation of sodium methyl sulfate, the smallest organosulfate,
564 Atmospheric Chemistry and Physics, 18, 2809-2820, 2018.
565 Lance, S., Medina, J., Smith, J. N., and Nenes, A.: Mapping the operation of the DMT Continuous Flow CCN counter,
566 Aerosol Science and Technology, 40, 242-254, 2006.
567 Lei, T., Zuend, A., Wang, W. G., Zhang, Y. H., and Ge, M. F.: Hygroscopicity of organic compounds from biomass
568 burning and their influence on the water uptake of mixed organic ammonium sulfate aerosols, Atmospheric
569 Chemistry and Physics, 14, 11165-11183, 2014.
570 Liao, J., Froyd, K. D., Murphy, D. M., Keutsch, F. N., Yu, G., Wennberg, P. O., St. Clair, J. M., Crounse, J. D.,
571 Wisthaler, A., Mikoviny, T., Jimenez, J. L., Campuzano-Jost, P., Day, D. A., Hu, W., Ryerson, T. B., Pollack, I. B.,
572 Peischl, J., Anderson, B. E., Ziemba, L. D., Blake, D. R., Meinardi, S., and Diskin, G.: Airborne measurements of
573 organosulfates over the continental US, Journal of Geophysical Research-Atmospheres, 120, 2990-3005, 2015.
574 Ma, Y., Xu, X., Song, W., Geng, F., and Wang, L.: Seasonal and diurnal variations of particulate organosulfates in
575 urban Shanghai, China, Atmospheric Environment, 85, 152-160, 2014.
576 Malm, W. C., and Kreidenweis, S. M.: The effects of models of aerosol hygroscopicity on the apportionment of
577 extinction, Atmos. Environ., 31, 1965-1976, 1997.
578 Marcolli, C., and Krieger, U. K.: Phase changes during hygroscopic cycles of mixed organic/inorganic model systems
579 of tropospheric aerosols, J. Phys. Chem. A, 110, 1881-1893, 2006.
580 McNeill, V. F., Woo, J. L., Kim, D. D., Schwier, A. N., Wannell, N. J., Sumner, A. J., and Barakat, J. M.: Aqueous-
581 Phase Secondary Organic Aerosol and Organosulfate Formation in Atmospheric Aerosols: A Modeling Study,
582 Environmental Science & Technology, 46, 8075-8081, 2012.
583 Moise, T., Flores, J. M., and Rudich, Y.: Optical properties of secondary organic aerosols and their changes by
584 chemical processes, Chem Rev, 115, 4400-4439, 2015.
585 Moore, R. H., Nenes, A., and Medina, J.: Scanning Mobility CCN Analysis-A Method for Fast Measurements of Size-
586 Resolved CCN Distributions and Activation Kinetics, Aerosol Science and Technology, 44, 861-871, 2010.
587 Noziere, B., Kaberer, M., Claeys, M., Allan, J., D'Anna, B., Decesari, S., Finessi, E., Glasius, M., Grgic, I., Hamilton,
588 J. F., Hoffmann, T., Iinuma, Y., Jaoui, M., Kahno, A., Kampf, C. J., Kourtchev, I., Maenhaut, W., Marsden, N.,
589 Saarikoski, S., Schnelle-Kreis, J., Surratt, J. D., Szidat, S., Szmigielski, R., and Wisthaler, A.: The Molecular
590 Identification of Organic Compounds in the Atmosphere: State of the Art and Challenges, Chemical Reviews, 115,
591 3919-3983, 2015.
592 Pöschl, U.: Atmospheric aerosols: composition, transformation, climate and health effects, Angewandte Chemie
593 International Edition, 44, 7520-7540, 2005.
594 Peng, C., Jing, B., Guo, Y. C., Zhang, Y. H., and Ge, M. F.: Hygroscopic Behavior of Multicomponent Aerosols
595 Involving NaCl and Dicarboxylic Acids, The journal of physical chemistry. A, 120, 1029-1038, 2016.
596 Peng, C., Wang, Y., Wu, Z., Chen, L., Huang, R. J., Wang, W., Wang, Z., Hu, W., Zhang, G., Ge, M., Hu, M., Wang,
597 X., and Tang, M.: Tropospheric aerosol hygroscopicity in China, Atmos. Chem. Phys., 20, 13877-13903, 2020.
598 Petters, M. D., and Kreidenweis, S. M.: A single parameter representation of hygroscopic growth and cloud
599 condensation nucleus activity, Atmospheric Chemistry And Physics, 7, 1961-1971, 2007.
600 Petters, M. D., and Kreidenweis, S. M.: A single parameter representation of hygroscopic growth and cloud
601 condensation nucleus activity - Part 2: Including solubility, Atmospheric Chemistry and Physics, 8, 6273-6279,
602 2008.
603 Petters, M. D., Wex, H., Carrico, C. M., Hallbauer, E., Massling, A., McMeeking, G. R., Poulain, L., Wu, Z.,
604 Kreidenweis, S. M., and Stratmann, F.: Towards closing the gap between hygroscopic growth and activation for
605 secondary organic aerosol - Part 2: Theoretical approaches, Atmospheric Chemistry and Physics, 9, 3999-4009,
606 2009.

Petters, M. D., and Kreidenweis, S. M.: A single parameter representation of hygroscopic growth and cloud condensation nucleus activity - Part 3: Including surfactant partitioning, Atmospheric Chemistry and Physics, 13, 1081-1091, 2013.
Pitzer, K. S., and Mayorga, G.: Thermodynamics of electrolytes. 2. Activity and osmotic coefficients for strong electrolytes with one or both ions univalent, Journal of Physical Chemistry, 77, 2300-2308, 1973.
Prenni, A.: Water uptake of internally mixed particles containing ammonium sulfate and dicarboxylic acids, Atmos. Environ., 37, 4243-4251, 2003.
Riipinen, I., Rastak, N., and Pandis, S. N.: Connecting the solubility and CCN activation of complex organic aerosols: a theoretical study using solubility distributions, Atmospheric Chemistry and Physics, 15, 6305-6322, 2015.
Riva, M., Chen, Y., Zhang, Y., Lei, Z., Olson, N. E., Boyer, H. C., Narayan, S., Yee, L. D., Green, H. S., Cui, T., Zhang, Z., Baumann, K., Fort, M., Edgerton, E., Budisulistiorini, S. H., Rose, C. A., Ribeiro, I. O., RL, E. O., Dos Santos, E. O., Machado, C. M. D., Szopa, S., Zhao, Y., Alves, E. G., de Sa, S. S., Hu, W., Knipping, E. M., Shaw, S. L., Duvoisin Junior, S., de Souza, R. A. F., Palm, B. B., Jimenez, J. L., Glasius, M., Goldstein, A. H., Pye, H. O. T., Gold, A., Turpin, B. J., Vizuete, W., Martin, S. T., Thornton, J. A., Dutcher, C. S., Ault, A. P., and Surratt, J. D.: Increasing Isoprene Epoxydiol-to-Inorganic Sulfate Aerosol Ratio Results in Extensive Conversion of Inorganic Sulfate to Organosulfur Forms: Implications for Aerosol Physicochemical Properties, Environ Sci Technol, 53, 8682-8694, 2019.
Roberts, G. C., and Nenes, A.: A continuous-flow streamwise thermal-gradient CCN chamber for atmospheric measurements, Aerosol Science and Technology, 39, 206-221, 2005.
Shrivastava, M., Cappa, C. D., Fan, J., Goldstein, A. H., Guenther, A. B., Jimenez, J. L., Kuang, C., Laskin, A., Martin, S. T., Ng, N. L., Petaja, T., Pierce, J. R., Rasch, P. J., Roldin, P., Seinfeld, J. H., Shilling, J., Smith, J. N., Thornton, J. A., Volkamer, R., Wang, J., Worsnop, D. R., Zaveri, R. A., Zelenyuk, A., and Zhang, Q.: Recent advances in understanding secondary organic aerosol: Implications for global climate forcing, Reviews of Geophysics, 55, 509-559, 2017.
Staudt, S., Kundu, S., Lehmler, H.-J., He, X., Cui, T., Lin, Y.-H., Kristensen, K., Glasius, M., Zhang, X., Weber, R. J., Surratt, J. D., and Stone, E. A.: Aromatic organosulfates in atmospheric aerosols: Synthesis, characterization, and abundance, Atmospheric Environment, 94, 366-373, 2014.
Stokes, R. H., and Robinson, R. A.: INTERACTIONS IN AQUEOUS NONELECTROLYTE SOLUTIONS .I. SOLUTE-SOLVENT EQUILIBRIA, Journal of Physical Chemistry, 70, 2126-&, 1966.
Surratt, J. D., Gomez-Gonzalez, Y., Chan, A. W. H., Vermeylen, R., Shahgholi, M., Kleindienst, T. E., Edney, E. O., Offenberg, J. H., Lewandowski, M., Jaoui, M., Maenhaut, W., Claeys, M., Flagan, R. C., and Seinfeld, J. H.: Organosulfate formation in biogenic secondary organic aerosol, Journal of Physical Chemistry A, 112, 8345-8378, 2008.
Svenningsson, B., Rissler, J., Swietlicki, E., Mircea, M., Bilde, M., Facchini, M. C., Decesari, S., Fuzzi, S., Zhou, J., Monster, J., and Rosenorn, T.: Hygroscopic growth and critical supersaturations for mixed aerosol particles of inorganic and organic compounds of atmospheric relevance, Atmospheric Chemistry and Physics, 6, 1937-1952, 2006.
Tang, M., Cziczo, D. J., and Grassian, V. H.: Interactions of Water with Mineral Dust Aerosol: Water Adsorption, Hygroscopicity, Cloud Condensation, and Ice Nucleation, Chemical Reviews, 116, 4205-4259, 2016.
Tang, M., Chan, C. K., Li, Y. J., Su, H., Ma, Q., Wu, Z., Zhang, G., Wang, Z., Ge, M., Hu, M., He, H., and Wang, X.: A review of experimental techniques for aerosol hygroscopicity studies, Atmospheric Chemistry and Physics, 19, 12631-12686, 2019a.
Tang, M., Gu, W., Ma, Q., Li, Y. J., Zhong, C., Li, S., Yin, X., Huang, R.-J., He, H., and Wang, X.: Water adsorption and hygroscopic growth of six anemophilous pollen species: the effect of temperature, Atmospheric Chemistry and Physics, 19, 2247-2258, 2019b.
Tolocka, M. P., and Turpin, B.: Contribution of Organosulfur Compounds to Organic Aerosol Mass, Environmental Science & Technology, 46, 7978-7983, 2012.
Wang, K., Zhang, Y., Huang, R.-J., Wang, M., Ni, H., Kampf, C. J., Cheng, Y., Bilde, M., Glasius, M., and Hoffmann, T.: Molecular Characterization and Source Identification of Atmospheric Particulate Organosulfates Using Ultrahigh Resolution Mass Spectrometry, Environmental Science & Technology, 53, 6192-6202, 2019a.
Wang, Y., Hu, M., Guo, S., Wang, Y., Zheng, J., Yang, Y., Zhu, W., Tang, R., Li, X., Liu, Y., Le Breton, M., Du, Z., Shang, D., Wu, Y., Wu, Z., Song, Y., Lou, S., Hallquist, M., and Yu, J.: The secondary formation of organosulfates under interactions between biogenic emissions and anthropogenic pollutants in summer in Beijing, Atmospheric Chemistry and Physics, 18, 10693-10713, 2018.

Wang, Y., Ma, Y., Li, X., Kuang, B. Y., Huang, C., Tong, R., and Yu, J. Z.: Monoterpene and Sesquiterpene alpha-Hydroxy Organosulfates: Synthesis, MS/MS Characteristics, and Ambient Presence, Environ Sci Technol, 53, 12278-12290, 2019b.

Wang, Y., Hu, M., Wang, Y.-C., Li, X., Fang, X., Tang, R., Lu, S., Wu, Y., Guo, S., Wu, Z., Hallquist, M., and Yu, J. Z.: Comparative Study of Particulate Organosulfates in Contrasting Atmospheric Environments: Field Evidence for the Significant Influence of Anthropogenic Sulfate and NOx, Environmental Science & Technology Letters, 2020.

Wang, Y., Zhao, Y., Wang, Y., Yu, J. Z., Shao, J., Liu, P., Zhu, W., Cheng, Z., Li, Z., Yan, N., and Xiao, H.: Organosulfates in atmospheric aerosols in Shanghai, China: seasonal and interannual variability, origin, and formation mechanisms, Atmos. Chem. Phys., 21, 2959-2980, 2021.

Wex, H., Petters, M., Carrico, C., Hallbauer, E., Massling, A., McMeeking, G., Poulain, L., Wu, Z., Kreidenweis, S., and Stratmann, F.: Towards closing the gap between hygroscopic growth and activation for secondary organic aerosol: Part 1–Evidence from measurements, Atmospheric Chemistry and Physics, 9, 3987-3997, 2009.

Wexler, A. S., and Clegg, S. L.: Atmospheric aerosol models for systems including the ions H+, NH4+, Na+, SO42-, NO3-,Cl-, Br-, and H2O, J. Geophys. Res., 107, 2002.

Wiedensohler, A., Birmili, W., Nowak, A., Sonntag, A., Weinhold, K., Merkel, M., Wehner, B., Tuch, T., Pfeifer, S., Fiebig, M., Fjaraa, A. M., Asmi, E., Sellegri, K., Depuy, R., Venzac, H., Villani, P., Laj, P., Aalto, P., Ogren, J. A., Swietlicki, E., Williams, P., Roldin, P., Quincey, P., Hueglin, C., Fierz-Schmidhauser, R., Gysel, M., Weingartner, E., Riccobono, F., Santos, S., Gruening, C., Faloon, K., Beddows, D., Harrison, R. M., Monahan, C., Jennings, S. G., O'Dowd, C. D., Marinoni, A., Horn, H. G., Keck, L., Jiang, J., Scheckman, J., McMurry, P. H., Deng, Z., Zhao, C. S., Moerman, M., Henzing, B., de Leeuw, G., Loeschau, G., and Bastian, S.: Mobility particle size spectrometers: harmonization of technical standards and data structure to facilitate high quality long-term observations of atmospheric particle number size distributions, Atmospheric Measurement Techniques, 5, 657-685, 2012.

Wise, M. E., Surratt, J. D., Curtis, D. B., Shilling, J. E., and Tolbert, M. A.: Hygroscopic growth of ammonium sulfate/dicarboxylic acids, Journal Of Geophysical Research-Atmospheres, 108, 2003.

Wu, Z. J., Nowak, A., Poulain, L., Herrmann, H., and Wiedensohler, A.: Hygroscopic behavior of atmospherically relevant water-soluble carboxylic salts and their influence on the water uptake of ammonium sulfate, Atmospheric Chemistry and Physics, 11, 12617-12626, 2011.

Zardini, A. A., Sjogren, S., Marcolli, C., Krieger, U. K., Gysel, M., Weingartner, E., Baltensperger, U., and Peter, T.: A combined particle trap/HTDMA hygroscopicity study of mixed inorganic/organic aerosol particles, Atmospheric Chemistry and Physics, 8, 5589-5601, 2008.

Zhang, Y.-Q., Chen, D.-H., Ding, X., Li, J., Zhang, T., Wang, J.-Q., Cheng, Q., Jiang, H., Song, W., Ou, Y.-B., Ye, P.-L., Zhang, G., and Wang, X.-M.: Impact of anthropogenic emissions on biogenic secondary organic aerosol: observation in the Pearl River Delta, southern China, Atmospheric Chemistry and Physics, 19, 14403-14415, 2019.